ERL-0301-TR

AR-003-732

DEPARTMENT OF DEFENCE

DEFENCE SCIENCE AND TECHNOLOGY ORGANISATION

ELECTRONICS RESEARCH LABORATORY

DEFENCE RESEARCH CENTRE SALISBURY
SOUTH AUSTRALIA

TECHNICAL REPORT

ERL-0301-TR

SKYWAVE RADAR DETECTABILITY OF VOLCANIC AEROSOLS

S.J. ANDERSON

Approved for Public Release

AUGUST 1984

COPY No. 14

AR-003-732

DEPARTMENT OF DEFENCE

DEFENCE SCIENCE AND TECHNOLOGY ORGANISATION

ELECTRONICS RESEARCH LABORATORY

TECHNICAL REPORT

ERL-0301-TR

SKYWAVE RADAR DETECTABILITY OF VOLCANIC AEROSOLS

S.J. Anderson

S U M M A R Y

During 1982 there occurred several incidents in which commercial jet aircraft suffered engine failure over Indonesia as they passed through clouds of dust injected into the stratosphere by an erupting volcano on Java. This paper presents some theoretical estimates of the detectability of such clouds using skywave radar. The results imply that detection would not be possible with the JINDALEE Stage B radar.

POSTAL ADDRESS: Director, Electronics Research Laboratory,
Box 2151, GPO, Adelaide, South Australia, 5001.

TABLE OF CONTENTS

LIST OF TABLES

LIST OF FIGURES

7. SAGE and Lidar measurements of Soufriere Plumes(ref.4)

8. Mean number of particles with diameters exceeding d(ref.8)

9. Mean relative mass of particles in equal logarithmic diameter intervals(ref.8)

10. Times of fall of particles of different sizes(ref.9)

11. Temperature - height profiles of the US Standard Atmosphere 1962(ref.10)

12. Typical electron density profiles(ref.11)

13. Variation of diatomic ion concentrations relative to 0^+(ref.12)

14. Daytime electron and ion temperature profiles(ref.10)

15. Vertical distribution of several neutral and ion species(ref.11)

16. Positive ion densities for day and night(ref.10)

1. INTRODUCTION

On 24 June 1982 a Boeing 747 operated by British Airways suffered engine failure at 35 000 ft over Indonesia after flying through volcanic dust injected into the atmosphere by Mt Galunggung, a 7500 ft volcano located in SW Java, which had been erupting intermittently since 5 April 1982. Subsequently, on 14 July 1982, a Singapore Airlines Boeing 747 experienced failure of two engines and overheating of a third when it encountered dust at 39 000 ft. The air route concerned lies partly within the coverage of the JINDALEE Stage B radar and the question arises: could the JINDALEE radar detect or infer the presence of volcanic dust clouds so as to alert air traffic to possible hazards?

There are several ways in which volcanic eruptions could conceivably modify the physical environment as observed by a skywave radar. The most apparent of these are:

(i) injection of volcanic material into the upper atmosphere where it could reflect skywave radar signals via the Rayleigh scattering mechanism;

(ii) physical and chemical processes involving volcanic dust whereby the normal ionic equilibria in the upper atmosphere are upset to the point where the refractive index is appreciably altered;

(iii) generation of acoustic-gravity waves which could propagate to ionospheric heights where they would manifest themselves as travelling ionospheric disturbances.

Of these only (i) and (ii) are relevant to the detection of dust clouds.

This note presents some rough estimates of the magnitudes and hence the significance of these mechanisms.

2. CHARACTERISTICS OF VOLCANIC AEROSOLS

2.1 Composition

Individual volcanoes vary significantly in the composition of their ejecta but the fine, particulate tephra fall predominantly into four classes(ref.1):

(a) lithic fragments - particles of the rock which made up the summit of the volcano prior to eruption;

(b) pumice - a rock froth formed by the rapid quenching of magma, composed of volcanic glass, crystals of several different minerals, and gas bubble voids;

(c) crystals and crystal fragments of various minerals which were derived from lithic fragments as well as from the crystallising magma; and

(d) shards of volcanic glass broken from the frothy magma.

The most important volcanic sources of high altitude contamination are the so-called "Plinian" eruptions, that is, gas-rich, sustained explosive eruptions with exceptionally high ($>$ 10 km) eruption columns (Table 1). For example, the plinian eruption column was the principal means of transporting particles and gases into the stratosphere during the 18 May 1980 eruption of Mount St Helens (Tables 2 to 4).

The gases and nonsilicate aerosol particles contained in the plinian column have six possible sources:

(i) tropospheric air entrained by the ascending column;

(ii) geothermal fluids near the magma body;

(iii) vaporisation of ground water from melted snow, ice and rain;

(iv) reaction of vegetation with a cloud of hot ash and gas;

(v) gases released explosively from the silicate liquid in the erupted magma; and

(vi) gases released explosively from the silicate liquid in the magma that was not erupted.

2.2 Chemistry

The effects of the chemistry of volcanic emissions on the stratosphere and lower ionosphere are strongly dependent on the emission fluxes and the resulting transport processes. It appears that the most important chemical processes are:

(i) the chemical production of aerosols which affect the Earth's radiation budget; in particular the sulphur-containing gases and water vapour are important;

(ii) the chemical interaction of volcanic gases (and perhaps volcanic aerosol surfaces) with the free-radical ozone chemistry of the stratosphere. The important species are H_2O and SO_2 and perhaps reactive chlorine compounds, CO, and oxides of nitrogen.

Most of the emissions of sulphur compounds eventually form sulphate aerosols. The increasing dominance of sulphate particles over ash particles with time in the stratosphere can be explained by: (a) early scavenging of ash by the condensation of emitted water vapour to form rapidly settling ice crystals; (b) rapid settling of large ash-containing particles; and (c) continuing productions of sulphate by oxidation of sulphur gases.

2.3 Transport and dispersion

In the absence of strong, stable layers in the troposphere the eruption plume encounters no significant buoyant resistance to its upward progress until it passes about 12 km in altitude. Further penetration to heights up to 45 km has been noted but 25 km is more typical (Tables 3 and 4; figure 1).

The subsequent evolution of the plume is obviously critically dependent on the stratospheric winds.

Inspection of SAGE satellite, lidar and jet impaction data(ref.2 to 4) suggests the preferential formation of thin laminar clouds due to wind shears (figures 2 to 4).

The trajectories of the clouds at different levels can meander, loop and diverge in a very complex fashion making prediction extremely difficult. This is evident in figures 5 and 6(ref.1). Attempts to model cloud evolution have not met with great success. For example, in the case of the Caribbean Soufriere eruptions in 1979, trajectories were calculated using a geostrophic

wind model based on NOAA geopotential maps, assuming that the injected material resided on the 70 mb surface(ref.4). While a qualitative agreement was found with subsequent plume positions over West Africa as observed by the SAGE satellite, the arrival times did not match. Further, airborne lidar measurements of optical extinction disagreed with the computed trajectory (figure 7). This discrepancy is variously attributed to the tendency of global maps to emphasise large-scale features of the flow fields and neglect local fluctuations, and to the fact that the geostrophic approximation appears to overestimate wind speeds when used closer to the equator than about 15° of latitude.

3. ESTIMATES OF AEROSOL EFFECTS

3.1 HF radar cross section

The scattering of electromagnetic waves from a tenuous distribution of small particles is an important problem which has attracted interest since Lord Rayleigh's original work in 1899.

Two distinct frameworks exist for dealing with "multiple scattering" phenomena: analytical theory and transport theory. Analytical theory begins with the underlying differential equations describing the field properties, introduces the scattering and absorption properties of the individual scatterers and then expresses the quantities of physical interest in terms of appropriate integral equations. These can then be solved by iterative or diagrammatic techniques. Transport theory deals directly with the flow of energy using the radiative transfer equation. A respectable attempt to calculate the transmission properties of a volcanic aerosol would require one of these approaches but time does not permit such an endeavour on this occasion. Instead the simpler problem of estimating the backscattering radar cross section is addressed. Owing to the extremely small dimensions of the aerosol particles it turns out that the result obtained here is equivalent to that which would result from the cumulative forward-scatter, single backscatter approximation of De Wolf(ref.5).

Consider the contribution to the backscattered field from one aerosol particle, assumed spherical. It can be shown (reference 6, page 510) that

$$E_S = - E_o \left[\frac{n^2 - 1}{n^2 + 2} \right] \frac{k^2 a^3}{R} e^{-ikR} \qquad (1)$$

with n the refractive index, a the radius and R the distance to the field point.

Defining the backscatter cross section σ_b by

$$\sigma_b \equiv \frac{4\pi R^2 |E_S|^2}{|E_o|^2}$$

The only information available about size distribution for this eruption is that the great majority of aerosol particles had $a < 100\ \mu m$ while about 1% of the mass was present in particles with $a < 1\ \mu m$.

From figure 9 a reasonable lower limit for a theoretical model of N(a) is $0.1\ \mu m$. Any errors in σ_b introduced by ignoring particles smaller than this are likely to be negligible given the a^6 weighting in equation (4). Hence the following constraints apply:

$$\int_{0.1\ \mu m}^{1\ \mu m} a^3 N(a)\ da = 10^{-2} \int_{0.1\ \mu m}^{100\ \mu m} a^3 N(a)\ da \tag{6}$$

$$\frac{4\pi\rho}{3} \int_{0.1\ \mu m}^{100\ \mu m} a^3 N(a)\ da \sim 5 \times 10^{-6}\ g\ cm^{-3}\ \text{(upper bound)} \tag{7}$$

These two equations suffice to specify a two parameter model of N(a). Physical considerations suggest a model of the form

$$\log N(a) - \alpha \log(a) = \beta \tag{8}$$

with α and β to be determined from equations (6) and (7), and this form is supported by the asymptotic distribution. Rewriting equation (8) in exponential form, substituting in equation (6) and integrating yields

$$a^{4+\alpha} \Big|_{10^{-7}}^{10^{-6}} = 10^{-2} . a^{4+\alpha} \Big|_{10^{-7}}^{10^{-4}} \tag{9}$$

provided $\alpha \neq -4$.

Analytic solution of this equation is nontrivial. Reasoning that the ratio of the ranges of integration of the two sides of equation (9) is about 10^{-2}, so the mass density should therefore be only a weak function of a implies that $\alpha \sim -3$. Using perturbation techniques leads to

$$\alpha = -3.024 \tag{10}$$

Substituting in equation (7),

$$N(a) = 3.58 \times 10^{-3}\ a^{-3.024}\ m^{-3}$$

Inserting equation (11) into equation (5) with D = 2 km and Ψ, the angle of elevation set to 6° yields

$$\sigma_{TOT} = 2.3 \times 10^{-15} \text{ m}^2 \quad (12)$$

This is the radar cross section for one square metre of aerosol measured normal to the propagation vector. Converting to ground coordinates and taking radar parameters appropriate for Mt Galunggung observed with the JINDALEE radar, the effective radar cross section per radar resolution cell becomes

$$\sigma_{eff} = 2.4 \times 10^{-8} \text{ m}^2 \quad (13)$$

This value is many orders of magnitude below detectability with a skywave radar.

It is interesting to note that with a microwave radar operating at 10 GHz, the radar cross section per unit volume of aerosol would be greater by a large factor:

$$\sigma_b \text{ (microwave)} \sim 6.25 \times 10^{10} \sigma_b \text{ (HF)} \quad (14)$$

If the beamwidth of the microwave radar were taken into account and integrations performed for more appropriate geometries, detection at sensible ranges might then be predicted by this theory. No effort has been applied to this problem.

3.2 Aerosol effects on ambient ionisation

Rayleigh scattering of radio waves from the volcanic aerosol, as discussed in Section 3.1, is the only available mechanism for skywave radar detection of dust clouds at the heights where they could pose a threat to aircraft. The mechanisms postulated in this section relate to phenomena which may occur at higher altitudes - over 50 or 60 km, say - and in general it would not be possible to infer reliably the presence of low altitude dust clouds from the observation of high altitude effects.

3.2.1 Enhanced recombination

The enduring volcanic aerosol distributions are concentrated in the lower stratosphere, well below the levels of strong ionisation (figure 12(ref.11)). Accordingly, the most likely mechanism for influencing radio wave propagation is modification of D-layer absorption via changes to the electron density.

At D-region heights the availability of three-body channels

$$X^+ + e + M \rightarrow X + M \quad (15)$$

and the presence of molecular ions with the degrees of freedom to undergo dissociative recombination

$$XY^+ + e \rightarrow X + Y \tag{16}$$

mean that electron loss mechanisms are not in short supply. Below 80 km altitude there are also multiply-hydrated proton complexes with a very high recombination coefficient approaching 10^{-5} cm^3 s^{-1}, compared with about 6 x 10^{-7} cm s^{-1} for NO^+ ions which dominate above 80 km (figure 13(ref.12)).

It follows that for aerosols to have a detectable effect some particularly efficient reaction would need to operate.

The reaction postulated here is catalytic recombination in which the surface of the aerosol particle provides a 100% efficient agency for the reactions

$$X^+ + A \rightarrow [X^+A] \tag{17}$$

$$[X^+A] + e \rightarrow [XA] \rightarrow X + A \tag{18}$$

and

$$e + Z \rightarrow Z^- \tag{19}$$

$$X^+ + Z^- \rightarrow X + Z \tag{20}$$

In order to estimate the rate constant for this process, assume the capture cross-section of the aerosol is equal to its physical cross-section. Since $T_e > T_i$ (figure 14) the inequality $v_e \gg v_i$ is ensured and hence the rate is governed by v_i. From simple kinetic theory considerations, for diatomic ions which dominate below 100 km (figure 15), the recombination coefficient is given by

$$\alpha^* = \pi \left[\frac{5\ kT_i}{3\ m_i}\right] N_i\ N_a\ .\ a^2 \tag{21}$$

where N_i and N_a are the ion and aerosol number densities.

Now $T_i \sim T_{neutral} \sim 3 \times 10^2$ °K while $a \leqslant 0.5\ \mu m$ above 40 km. The dominant ion species is NO^+ so $m_i = 30\ m_p$; $N_i \sim 10^5$ cm^{-3} at 90 km (figure 15) whence, at most,

$$\alpha^* \sim 2.9 \times 10^{-5}\ N_a\ cm^3\ s^{-1} \tag{22}$$

Thus, in order to be significant in competition with the dominant loss mechanisms below 80 km an aerosol particle density of over 1 cm^{-3} is required.

For altitudes in the range 20 to 40 km where aerosol number densities near 1 cm^{-3} could apply for 0.5 μm particles, N_i is at least two orders of magnitude less than it is at 90 km (figure 16). On the other hand, for altitudes near the D-E transition where $N_i \geqslant 10^5$ cm^{-3}, aerosol densities of 1 particle (of 0.5 μm radius) per cubic centimetre equate to a mass loading of 10^{-6} g cm^{-3} compared with an air density of about 10^{-7} g cm^{-3} (65 km) or 10^{-8} g cm^{-3} (83 km) (figure 11). In other words, the air is not dense enough to support the aerosol.

Since this hypothetical 100% efficient recombination mechanism could not produce observable effects, it is reasonable to assert that more realistic (and more complicated) mechanisms are unlikely to do so.

3.2.2 Capture of free electrons without recombination

Another hypothetical process which could be advanced as a possible agent for observable effects is preferential attachment whereby electrons are readily captured by aerosol particles according to equation (19) but, for some reason, recombination processes such as equation (20) are suppressed.

In the simple model proposed here, the aerosol particle accretes charge until electrostatic repulsion prevents further capture. This limit corresponds to a balance between the thermal energy of the electrons and the Conlomb potential on the aerosol surface:

$$\frac{3\ kT}{2} = \frac{Ne^2}{4\pi\epsilon_o a} \qquad (23)$$

At altitudes below 50 km the electron density is too low to allow appreciable absorption. For the upper D-region, $T_e \sim 10^3$ °K. Then the maximum number of charges which could be accumulated by a single particle is given by

$$N \sim 9 \times 10^7\ a \qquad (24)$$

where a is in metres.

Setting a = 0.2 μm which, from figure 8 seems a reasonable upper bound for aerosols above 50 km, leads to N = 18 electrons per particle. Now, for mid-D region and night-time E, electron densities of $\sim 10^3$ cm^{-3} are typical. It follows that if the aerosol density were to approach $\sim 10^2$ cm^{-3} a large fraction of the free electrons could be captured, thereby removing the main absorption mechanism without affecting the ionisation density. Such a density is not possible at a = 0.2 μm because the corresponding

mass loading is 6×10^{-8} g cm^{-3} which is $\sim 0.1\ \rho$(air) at 50 km but exceeds ρ(air) at 70 km.

If a were smaller, say 0.02 μm, the charge captured would decrease by one order of magnitude but there would be 10^3 more particles for the same density. Using a mass loading of 0.1% of the air density (equal to the mean value in the model of Section 3.1 based on Mount St Helens data) still leaves the depletion a factor of 10 too small to be significant at 70 km. Thus only a minor effect on absorption appears possible even when recombination processes are prohibited.

To place these absorption calculations further in perspective, pathloss experiments during the JINDALEE program indicate typical two-way absorption losses of about 6 dB(ref.13). Thus the most severe effect of a major reduction in non-deviative absorption is still essentially a threshold effect given the other variabilities which characterise skywave propagation.

3.2.3 Depletion of sporadic-E

There is no available data on aerosol densities at E-region heights but any reasonable extrapolation to 90 km and above yields exceedingly low concentrations of only the smallest particles. Thus ionisation modification of normal E-region plasma properties can safely be regarded as negligible. The only avenue which could conceivably lead to aerosol influence is interaction with sporadic-E (E_s).

Sporadic-E is believed to be due to the presence of long-lived metallic ions of mainly meteoric origin. The principle loss processes for these ions - mainly Mg^+, Na^+, Fe^+ and Ca^+ - is dissociative recombination via ion-exchange reactions, eg

$$Mg^+ + O_2 \rightarrow MgO^+ + O \qquad (25)$$

$$MgO^+ + e \rightarrow Mg + O \qquad (26)$$

The rate coefficients for reactions of this type are very low, $\sim 10^{-10}$ cm^3 s^{-1}(ref.14). It could be the case that active sulphated radicals produced from the volcanic aerosol provide a depletion mechanism for these metallic ions which is otherwise lacking, leading to the destruction of E_s layers. From the point of view of detection, however this is probably irrelevant since the stratospheric aerosols of concern to aircraft would not be correlated with the high altitude phenomena (eg figure 5). In any event, horizontal structure in E_s is usually so pronounced that observability and recognition of perturbed E_s would not be possible.

4. CONCLUSIONS

By means of the simple physical models developed in this paper, rough estimates have been derived for the magnitudes of several mechanisms whereby skywave radar might detect volcanic aerosols. The conclusion in each case is that detection is not viable.

In the case of direct radar echoes from the dust clouds, the calculated effects are many orders of magnitude too weak to be detectable. In contrast, some of the high altitude effects appear to be within one or two orders of magnitude of being observable, but these effects have been calculated for idealised hypothetical processes which may not occur in reality.

Microwave radar detectability of dust clouds could be computed by a simple extension of the model developed here for HF but this has not been attempted.

Postscript

On 3 February 1984 it was learned that Mt Galunggung was erupting. The JINDALEE radar was used in a variety of modes to observe the region around the volcano but no unusual echoes or fading could be detected.

REFERENCES

No.	Author	Title
1	Newell, R. and Deepak, A. (Eds)	"Mount St Helens Eruptions of 1980". Report of NASA Workshop, November 1980, US Govt Printing Office (1982)
2	Fujiwara, M. Itabe, T. and Hirono, M.	"Sudden Increase in Stratospheric Aerosol Content After the Eruption of Fuego Volcano; Lidar Observations in Fukuoka". Rep. Ionos. Space. Vol. 29, p.74 (1975)
3	Gras, J.L.	"Southern Hemisphere Mid-Latitude Stratospheric Aerosol after the 1974 Fuego Eruption". Geophys. Res. Lett. Vol. 3, p.533 (1976)
4	McCormick, M.P., Kent, G.S., Yue, G.K. and Cunnold, D.M.	"SAGE Measurements of the Stratospheric Aerosol Dispension and Loading from the Soufriere Volcano". NASA Technical Paper 1922 (1981)
5	De Wolf, D.A.	"Electromagnetic Reflection from an Extended Turbulent Medium". IEEE Trans. Ant. Prop. Vol. AP-19, p.254 (1971)
6	Jones, D.S.	"The Theory of Electromagnetism". Pergamon (1964)
7	Sinnott, D.H.	Private Communication (1983)
8	Bigg, E.K.	"Stratospheric Particles". J. Atmos. Sciences. Vol. 32, p.910 (1975)
9	Glasstone, S. and Delan, P.J.	"The Effects of Nuclear Weapons". US Govt. Printing Office (1977)
10	Valley, S.L. (Ed)	"Handbook of Geophysics and Space Environments". McGraw-Hill (1965)
11	Rishbeth, H.	"Physics and Chemistry of the Ionosphere". Contemp. Phys. Vol. 14, p.229 (1973)
12	Danilov, A.D.	"Chemistry of the Ionosphere". Plenum (1970)
13	Blesing, R.G.	Private communication (1983)
14	Ignat'ev, Y.A.	"The Action of Artificial Heating of the Ionosphere on the Inhomogeneous Structure of the E Region". Iz. Vyssh. Uch. Zav., Radiofizika, Vol. 21, p.357 (1978)

TABLE 1. COMPARISON OF 18 MAY ERUPTION OF MOUNT ST HELENS WITH OTHER ERUPTIONS(REF.1)

	Mount St Helens	Worldwide maximum past 250 years	Worldwide maximum all time
Total magma volume erupted, (expressed as cubic kilometres of dense rock)	0.5		> 1000
Eruption magnitude[a]	6		10
Eruption column height, (kilometres above volcano)	23 to 27 maximum 18 average	28 to 35[d]	40 +[d]
Duration of climax of eruption (hours)	9	38	48
Volcanic explosivity index (VEI)[b]	5	7	8
Area covered by isopach enclosing half volume of deposit (square kilometres)	1×10^5	6×10^4	10^6
Area of complete devastation (square kilometres)	500	1000	5×10^4 [c]

[a] Tsuya (1955).

[b] Newhall and Self (1982).

[c] Walker (1980).

[d] > 40 km supposedly reached by Krakatoa, 1883 and Bezymianny, 1956: both inadequately substantiated.

TABLE 2. ESTIMATES OF VOLATILES RELEASED BY THE 18 MAY ERUPTION (REF. 1)

Mass of magma erupted at Mount St Helens

18 May volume[a]	0.3 km^3
post-18 May volume	0.03 km^3
Total	0.33 km^3

Initial content[b]

S	$<$ 500 ppm
Cl	1000 ppm
H_2O	5 wt. %

Minimum volatiles erupted

S	(0.33) km^3) (250 ppm) (2.4 g/cc) x 10^{15}	=	2 x 10^{11} g
Cl	(0.33) km^3) (1000 ppm) (2.4 g/cc) x 10^{15}	=	0.8 x 10^{12} g
H_2O	(0.33) km^3) (5%) (2.4 g/cc) x 10^{11}	=	4 x 10^{14} g

These values assume:

(a) no meteoric, hydrothermal, or atmospheric water;

(b) no scavenging;

(c) complete degassing; and

(d) no contribution from intrusive magma.

Estimates of atmospheric impact will have to consider and evaluate these factors.

[a] Value is uncertain, between 0.2 and 0.5 km^3.

[b] Values based on data of Melson et al (1980). Note particularly the uncertainty for S.

TABLE 3. ERUPTION RATES AND COLUMN HEIGHTS FOR SOME RECENT VOLCANIC ERUPTIONS(REF.1)

	Maximum volume flux rate (m^3/s dense rock)	Maximum column height (kilometres) above volcano[a]
Mount St Helens, 1980	2×10^4	22(o)
Hekla, 1947	2×10^4	24(o),21(c)
Agung, 1963	3×10^4	23(c)
Bezymianny, 1956	2×10^5	45(o),42(c)
Santa Maria, 1902	4×10^4	34(c),29(o)
Hekla, 1970	6×10^3	16(o),15(c)
Ngauruhoe, 1975[b]	2×10^3	10(o),10(c)
Taupo, 160 AD	1×10^6	> 50(c)

[a] o = observed, c = calculated.

[b] A vulcanian (less intense than plinian) eruption.

TABLE 4. MAXIMUM HEIGHTS OF ERUPTION COLUMNS AT MOUNT ST HELENS(REF.1)

Date of eruption	Maximum column heights (kilometres)	Duration of ash emission at elevations above 12 km
18 May	> 24.4, 17.3, 14.6, 19.2	about 9 hours
25 May	12.2	less than 30 min
12 June	15.2, 10.7, 9.8, 10.7	about 30 min
22 July	13.7, 14.5, 13.7	25 min
7 August	13.4, 10.0, 6.1, 7.6, 5.2	2 to 5 min
16 October	12.8	less than 5 min
17 October	14.3, 13.7	less than 5 min
18 October	5.2, 7.9	less than 5 min

[1]From Harris et al, 1981a.

TABLE 5. VOLUMES OF SOME RECENT AIRFALL DEPOSITS(REF.1)

Volcanic eruption	Volume (cubic kilometres of dense rock)
Mount St Helens, 1980	0.2 to 0.48
Fuego, 1970	0.1
Agung, 1963	0.6 to 1.2 (March and May events)
Bezymianny, 1956	0.5 to 2.0
Hekla, 1947	0.3
Santa Maria, 1902	4 to 9
Krakatoa, 1883	5 to 10
Tambora, 1815	30 (very approximate)
Taupo, 160 AD	6 to 10

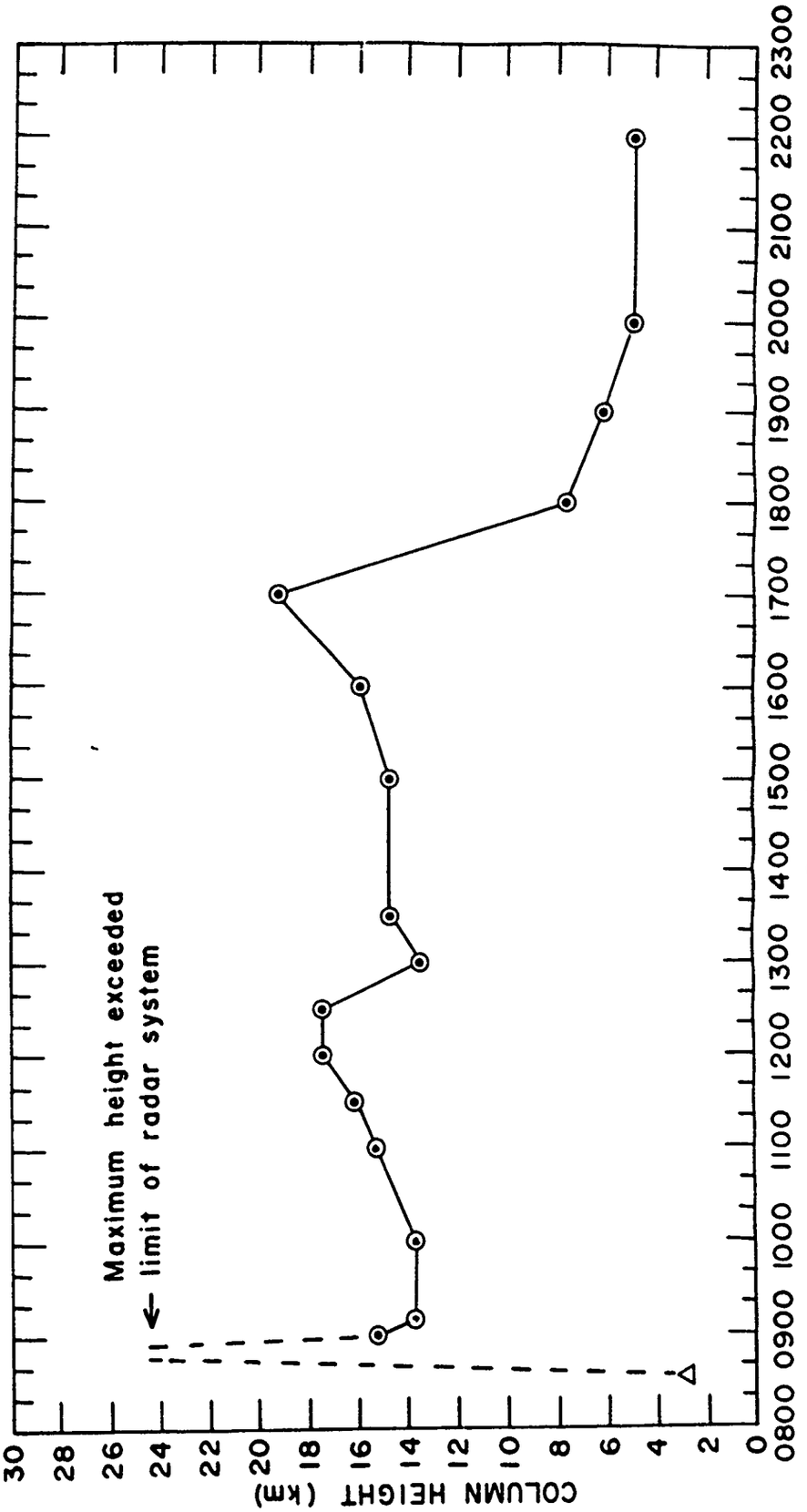

Figure 1. Time dependence of the Plinian Column for the Mount St Helens eruption of 18 May 1980(ref.1)

ERL-0301-TR
Figure 2

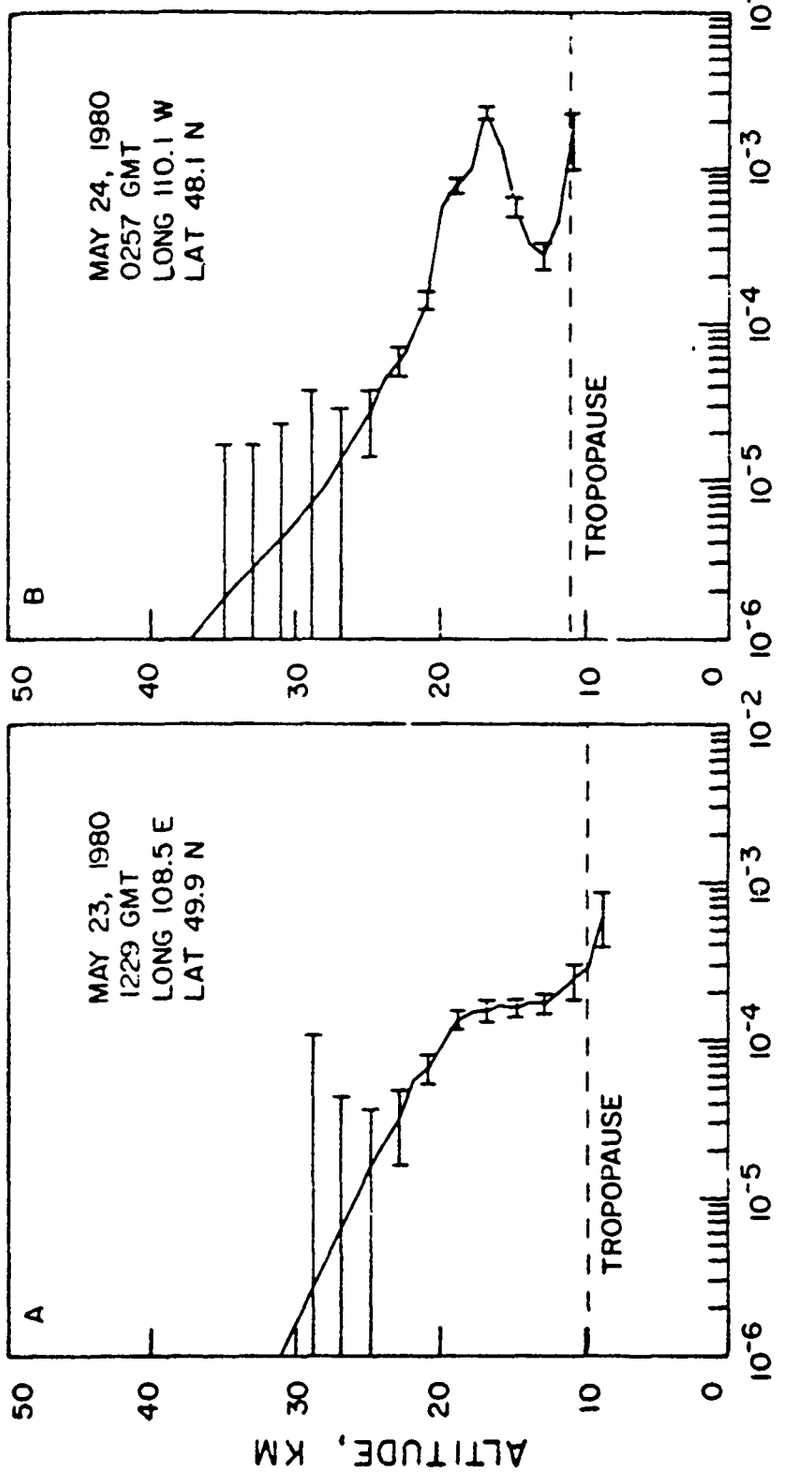

Figure 2. Stratospheric aerosol extinction rates measured by SAGE(ref.4)

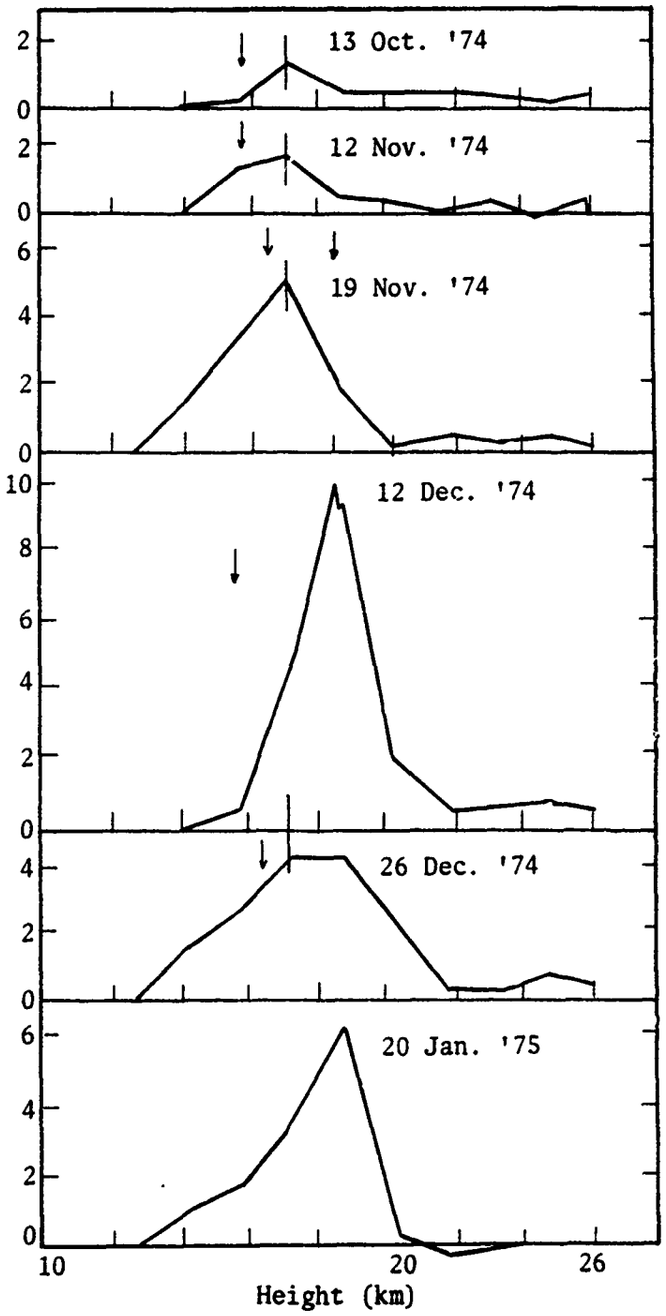

Figure 3. Lidar Non-Rayleigh backscattering coefficient profile(ref.2)

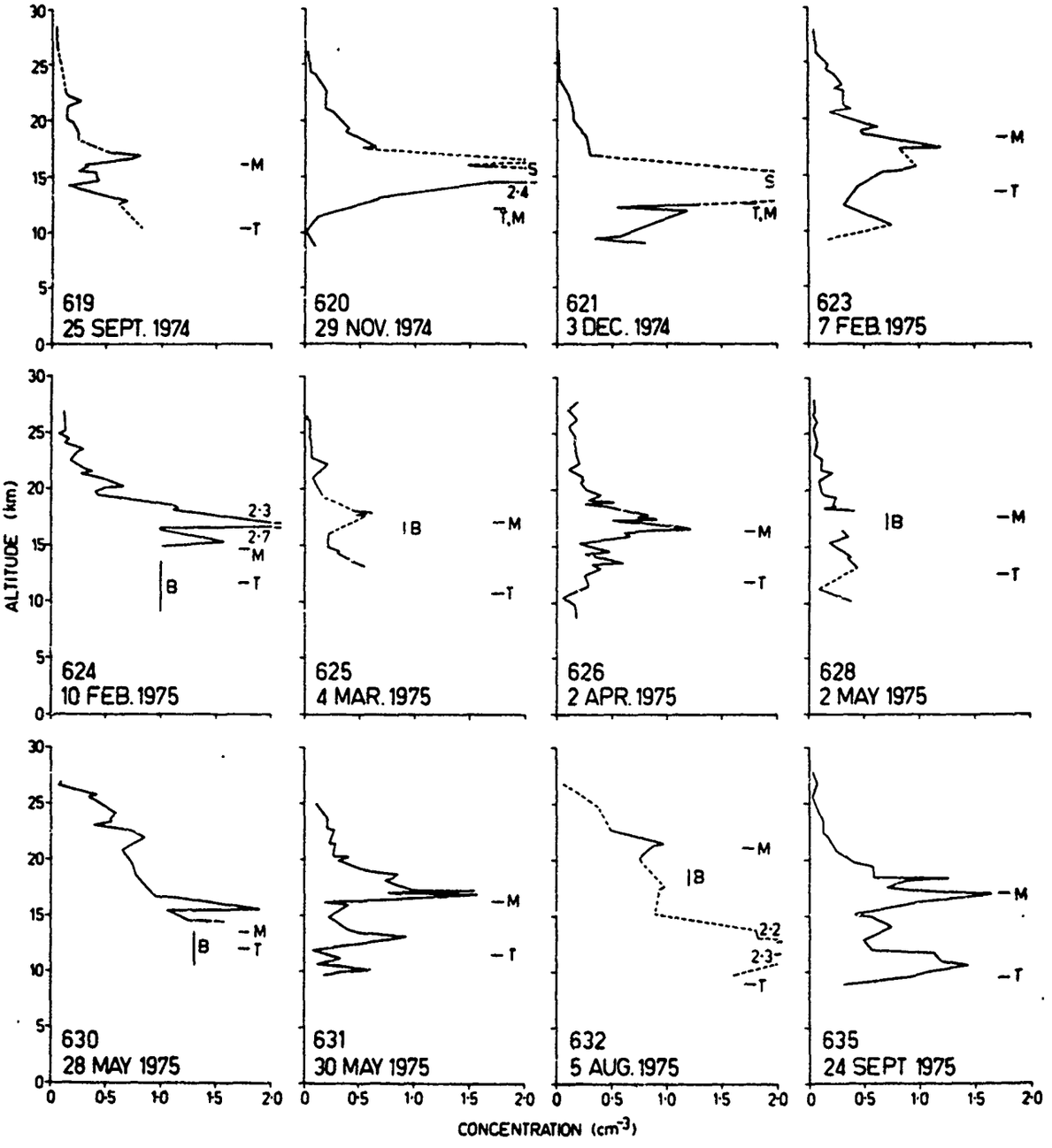

Figure 4. Profiles of aerosol number concentration(ref.3)

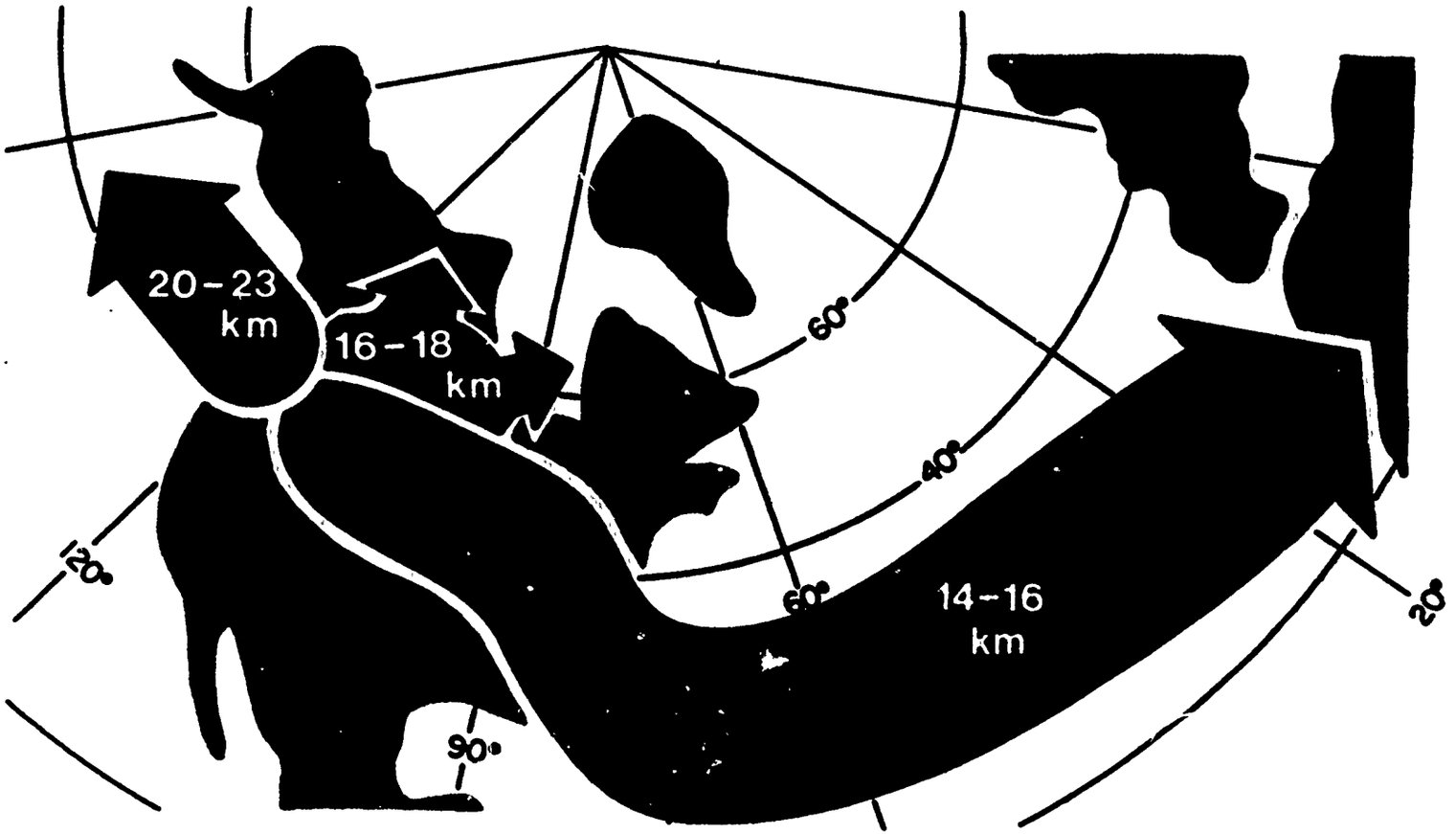

Figure 5. SAGE map of stratospheric aerosol distribution(ref.1)

ERL-0301-TR
Figure 5

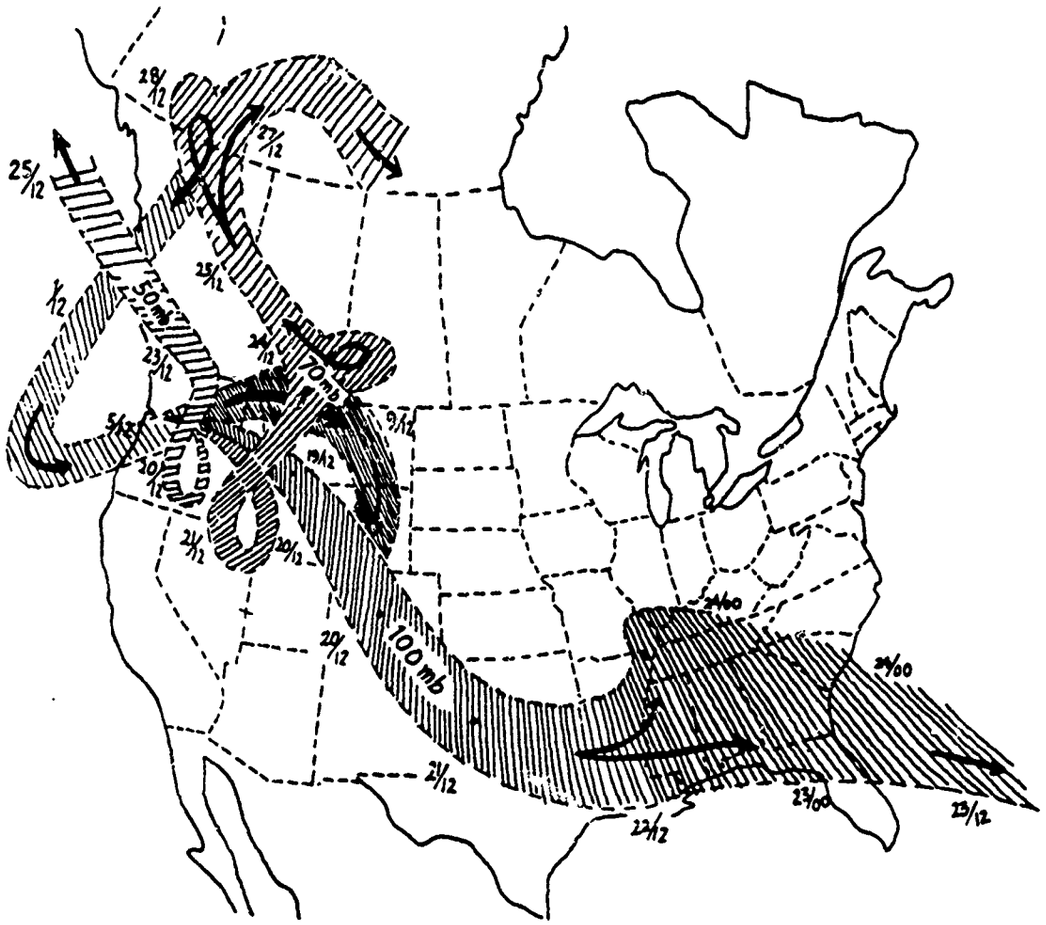

Figure 6. Trajectories for the 18 May eruption(ref.1)

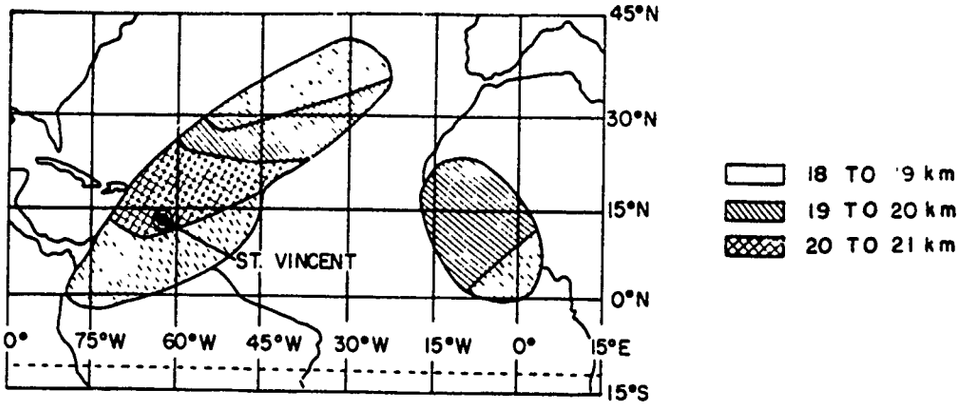

(a) Map showing areas and altitudes of enhanced extinction (50 percent or more above normal) as observed by SAGE between April 21 and 28, 1979.

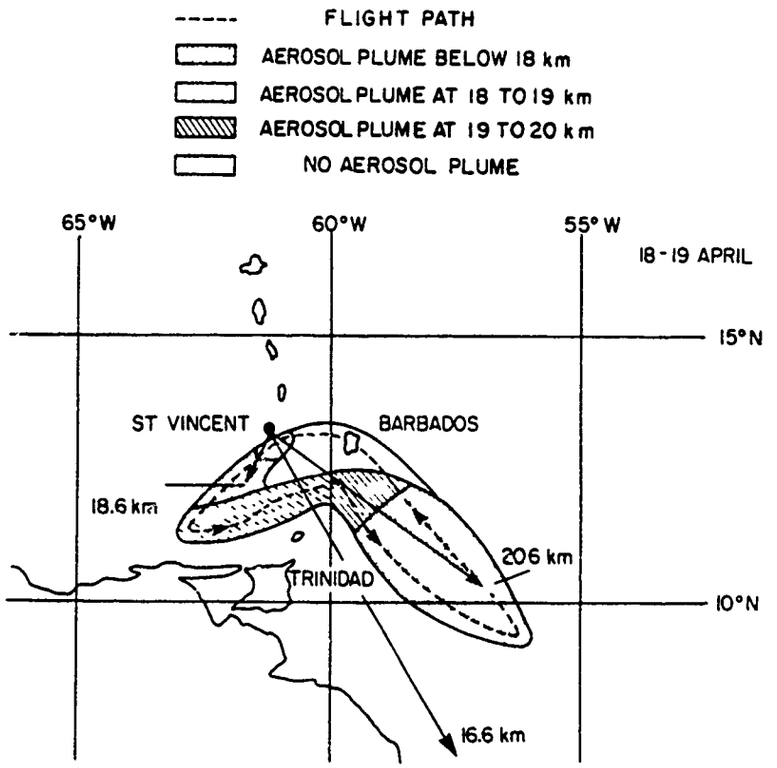

(b) Airborne lidar observations in the vicinity of St. Vincent, April 18 and 19, 1979. Also shown are the calculated air movements at three pressure levels during the interval between the eruption at 2057 GMT on April 17, 1979, and the time of the flight.

Figure 7. SAGE and Lidar measurements of Soufriere Plumes(ref.4)

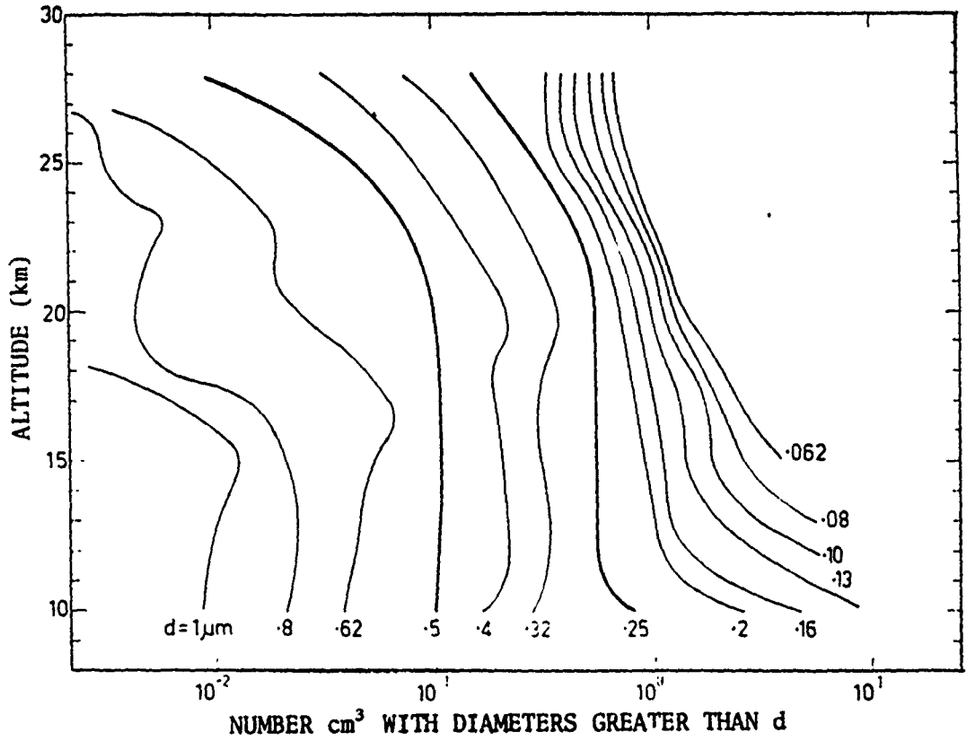

Figure 8. Mean number of particles with diameters exceeding d(ref.8)

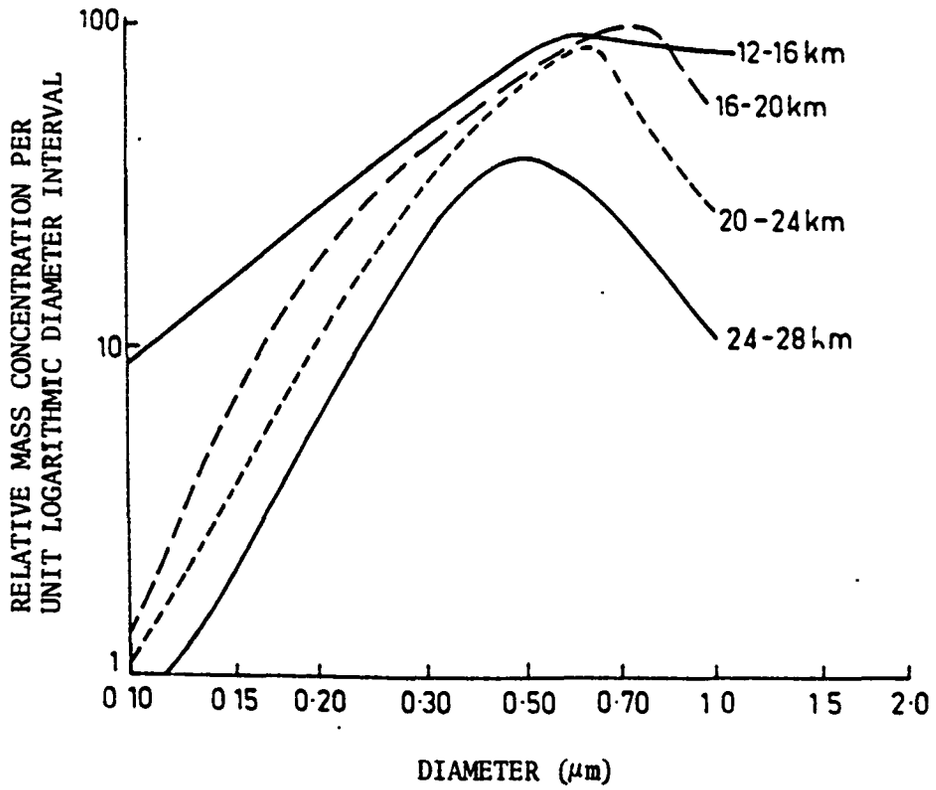

Figure 9. Mean relative mass of particles in equal logarithmic diameter intervals(ref.8)

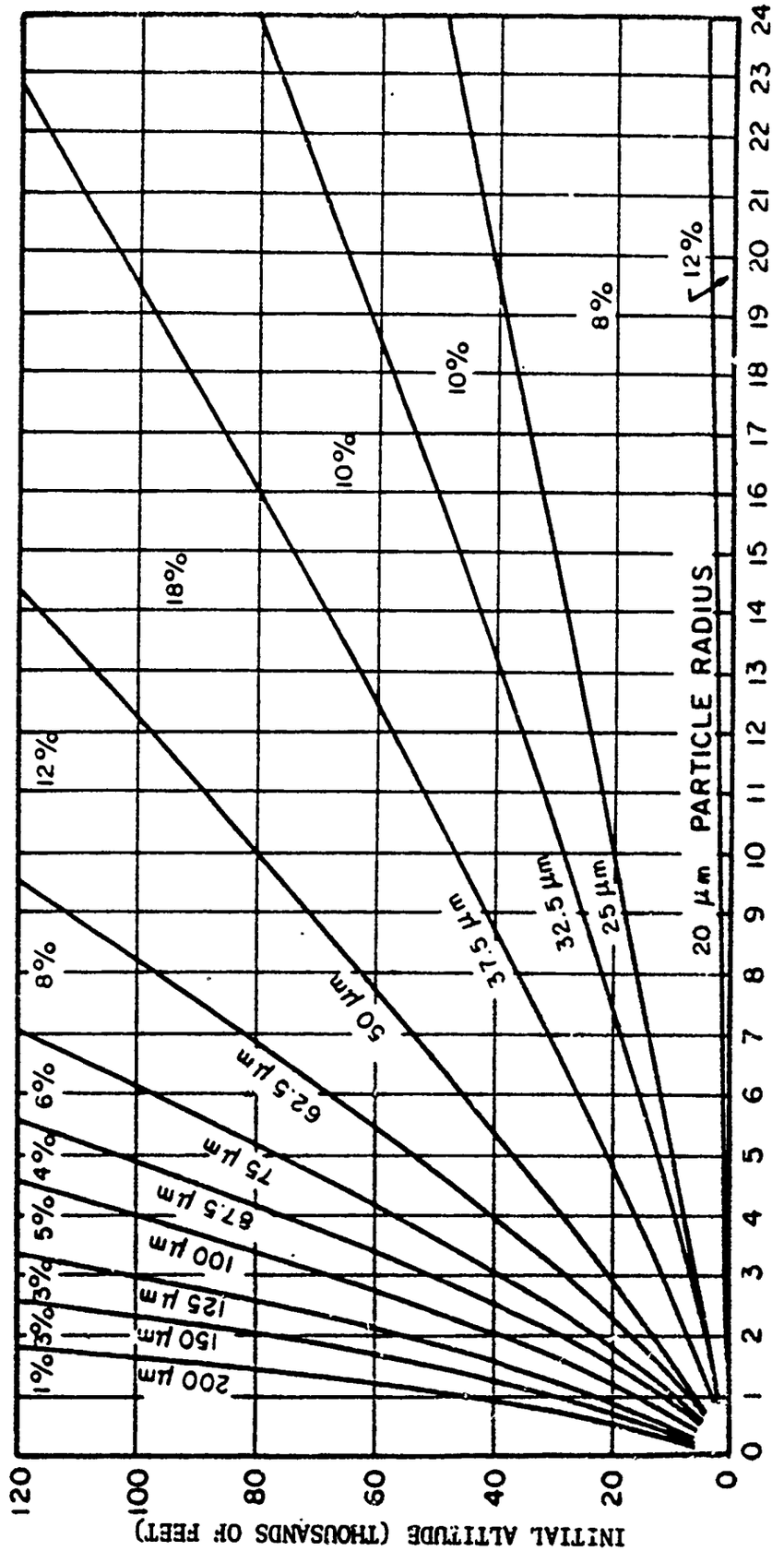

Figure 10. Times of fall of particles of different sizes(ref.9)

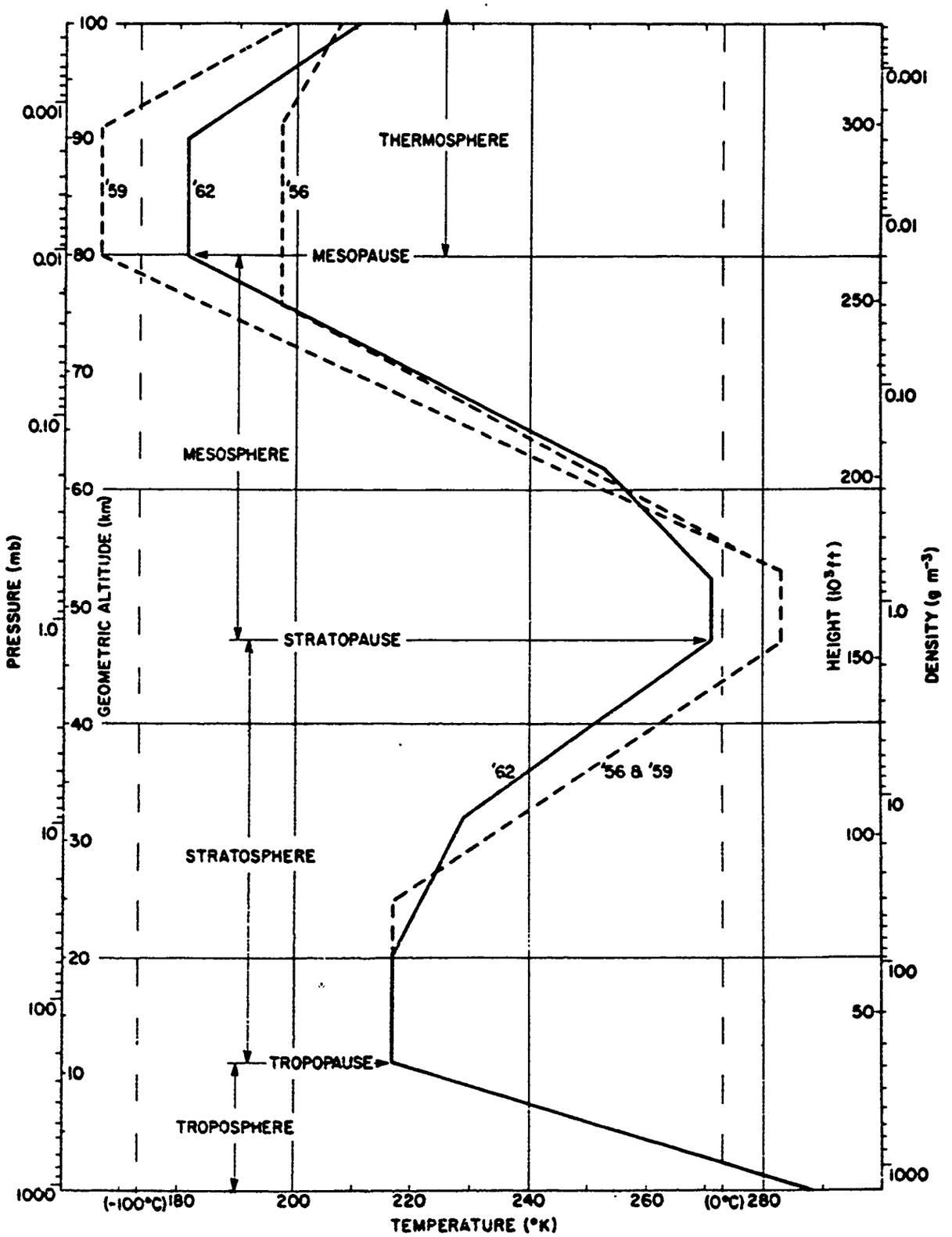

Figure 11. Temperature - height profiles of the US Standard Atmosphere 1962(ref.10)

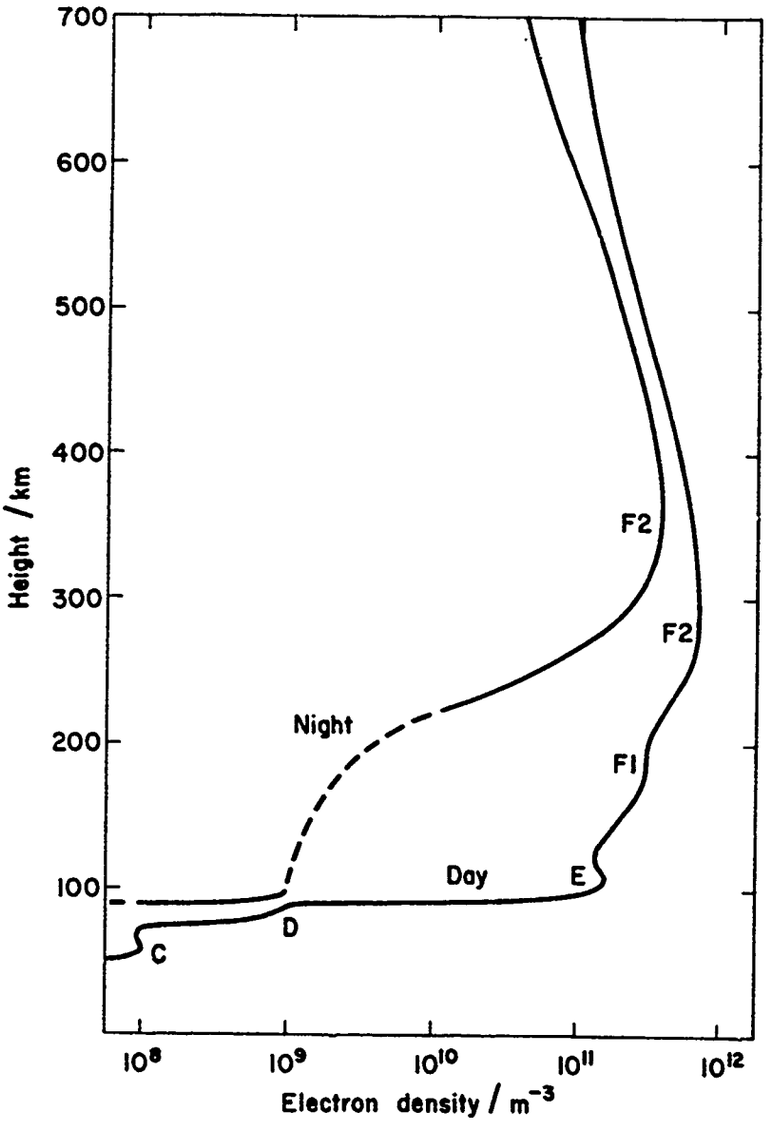

Figure 12. Typical electron density profiles(ref.11)

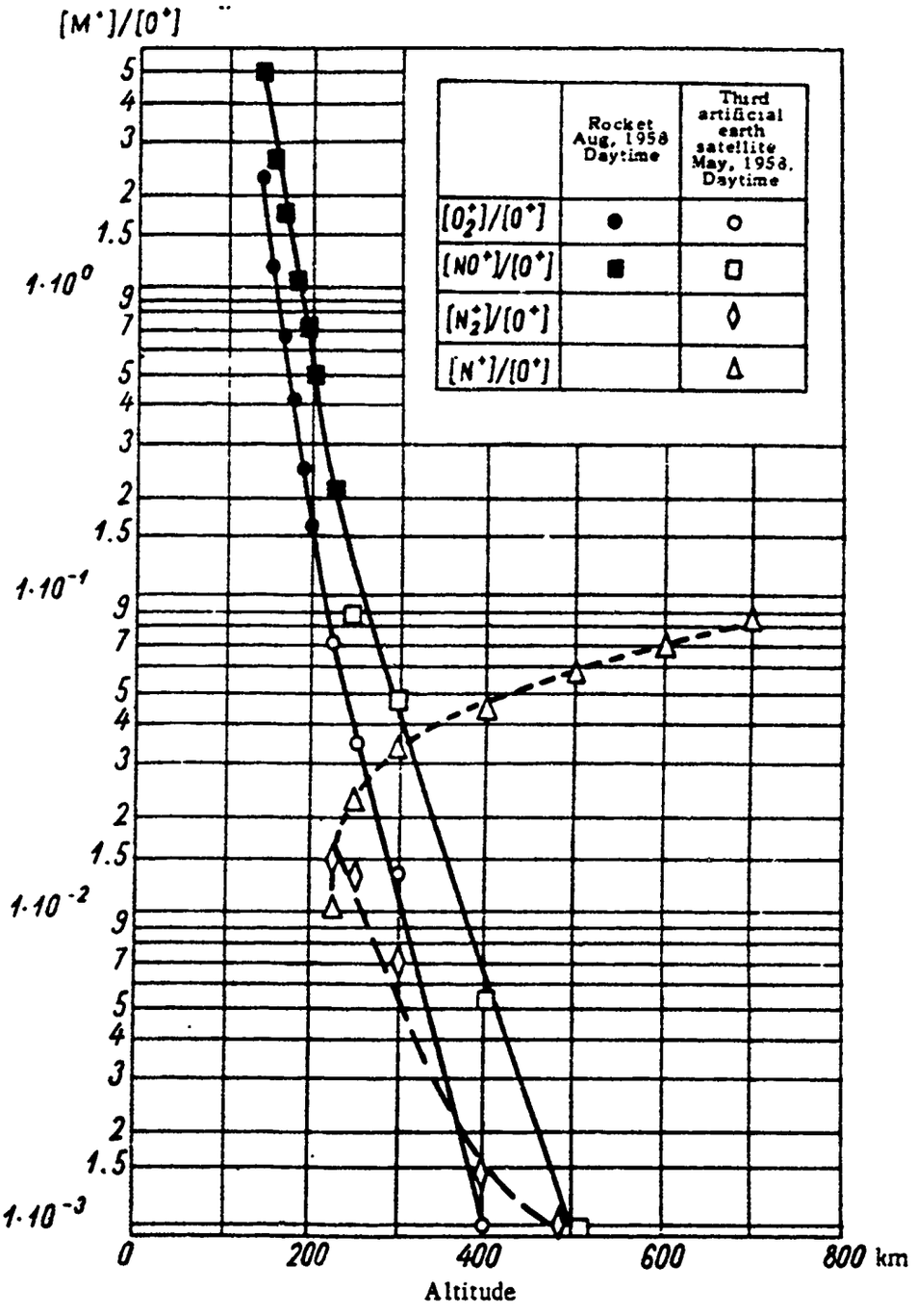

Figure 13. Variation of diatomic ion concentrations relative to O^+(ref.12)

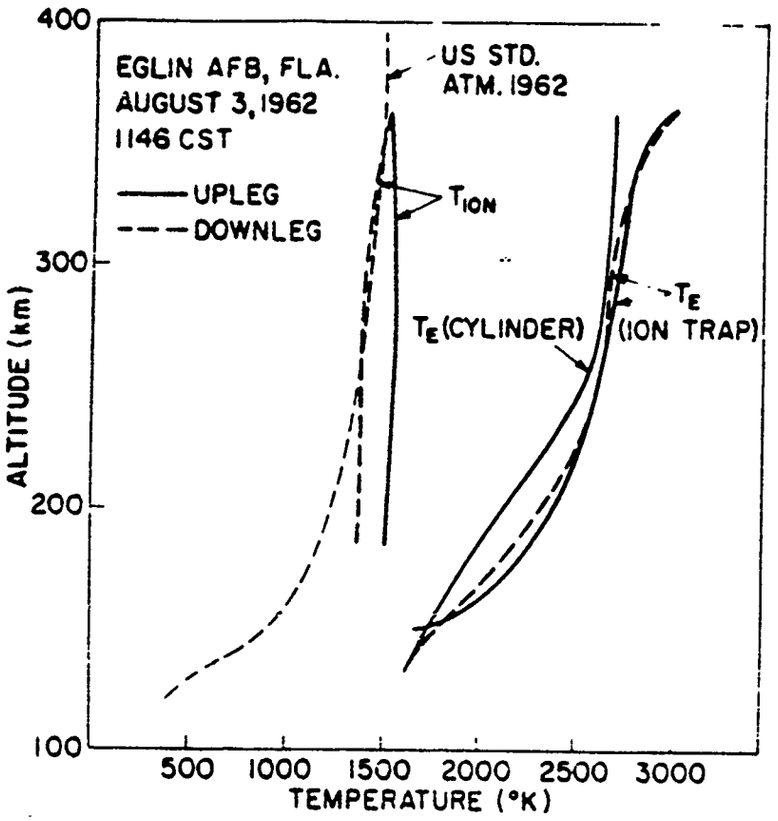

Figure 14. Daytime electron and ion temperature profiles(ref.10)

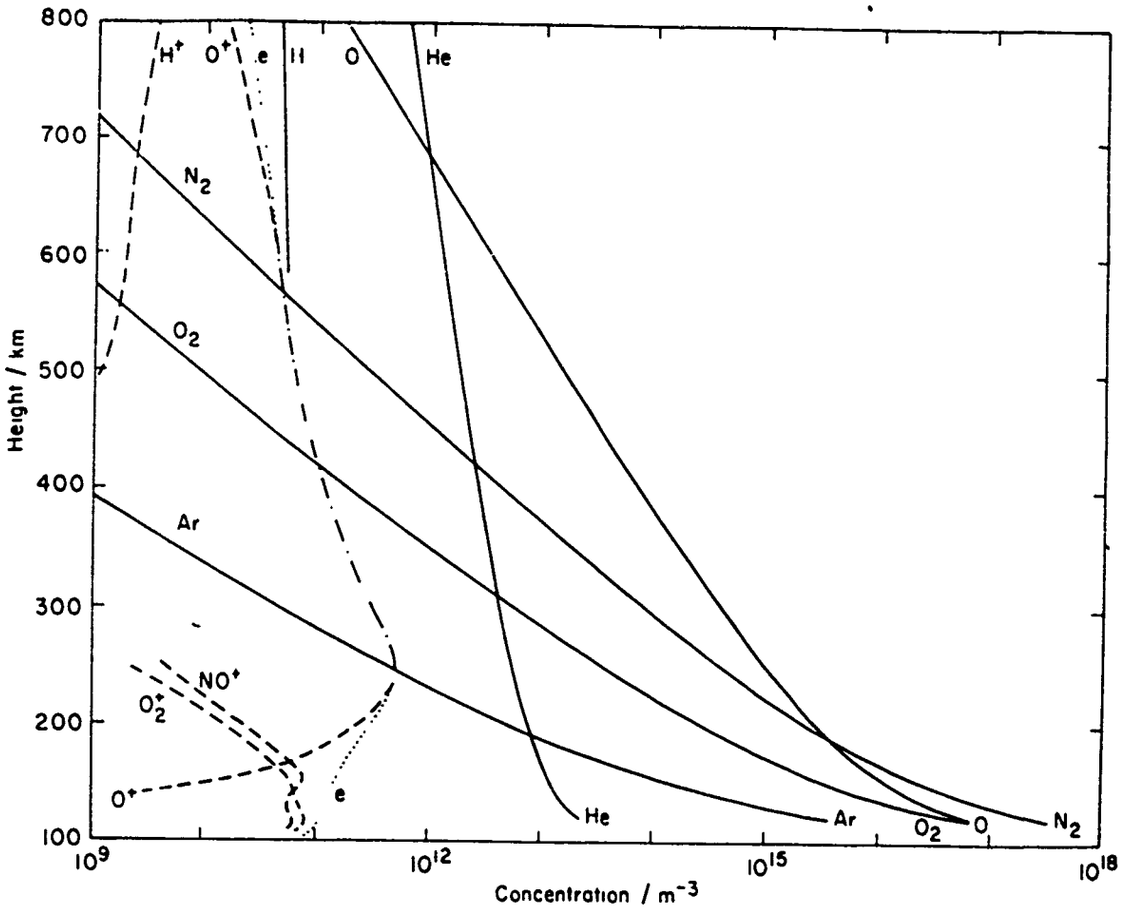

Figure 15. Vertical distribution of several neutral and ion species(ref.11)

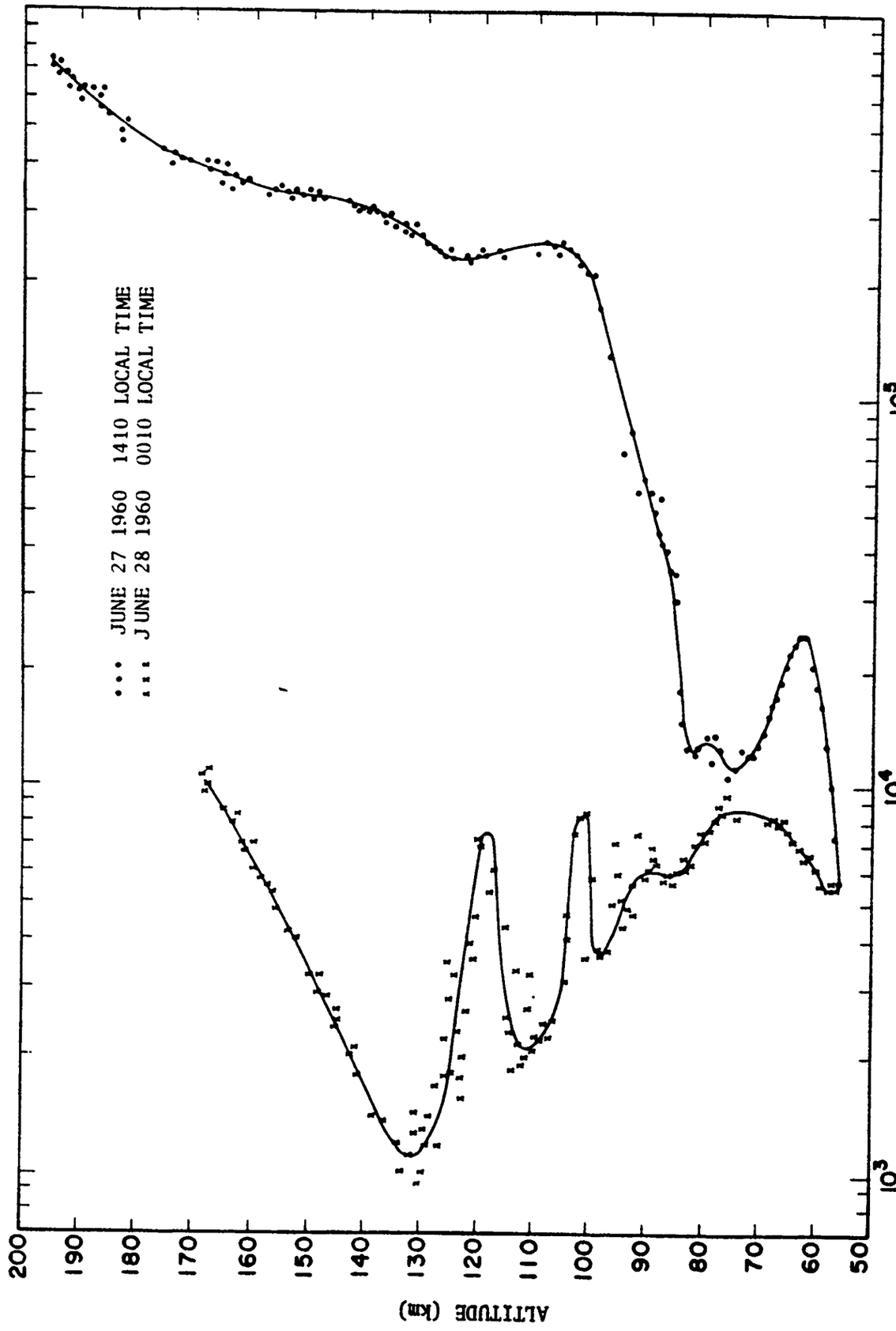

Figure 16. Positive ion densities for day and night(ref.10)

DISTRIBUTION

	Copy No.
EXTERNAL	
In United Kingdom	
Defence Science Representative, London	Cnt Sht Only
British Library, Lending Division	1
Institution of Electrical Engineers	2
In United States of America	
Counsellor, Defence Science, Washington	Cnt Sht Only
Engineering Societies Library	3
In Australia	
Department of Defence	
Chief Defence Scientist	4
Deputy Chief Defence Scientist	
Superintendent, Science Programs and Administration	
Controller, External Relations, Projects and Analytical Studies	
Air Force Scientific Adviser	5
Navy Scientific Adviser	Cnt Sht Only
Director, Joint Intelligence Organisation	6
Document Exchange Centre Defence Information Services Branch for:	
Microfilming	7
United Kingdom, Defence Research Information Centre (DRIC)	8 - 9
United States, Defense Technical Information Center	10 - 21
Canada, Director, Scientific Information Services	22
New Zealand, Ministry of Defence	23
National Library of Australia	24

Director General, Army Development (NSO), Russell Offices for ABCA Standardisation Officers	
UK ABCA representative, Canberra	25
US ABCA representative, Canberra	26
Canada ABCA representative, Canberra	27
NZ ABCA representative, Canberra	28
Defence Library, Campbell Park	29
Library, Aeronautical Research Laboratories	30
Library, Materiels Research Laboratories	31
Library, H Block, Victoria Barracks, Melbourne	32
Library, RAN Research Laboratory	33
Department of Defence Support	
Deputy Secretary (Manufacturing)	34
Deputy Secretary (Materiel and Resources)	
Controller, Defence Aerospace Division	
Controller, Munitions Division	
Library, DDS Central Office	35
Director, Industry Development, SA/NT	Cnt Sht Only
WITHIN DRCS	
Director, Electronics Research Laboratory	36
Director, Weapons Systems Research Laboratory	37
Superintendent, Radar Division	38
Principal Officer, Microwave Radar Group	39
Principal Officer, Radio Group	40
Principal Officer, Jindalee Development Group	41
Principal Officer, Jindalee Project Group	42
Dr M.G. Golley, Jindalee Project Group	43
Dr G.F. Earl, Jindalee Project Group	44
Dr S.J. Anderson, Jindalee Development Group	45
DRCS Library	46 - 47
Spares	48 - 49

Security classification of this page: UNCLASSIFIED

13 ANNOUNCEMENT LIMITATIONS (of the information on these pages):

No Limitation

14 DESCRIPTORS:			15 COSATI CODES
a. EJC Thesaurus Terms	Skywave radar Over-the-horizon radar Volcanoes Aerosols Over-the-horizon detection	Volcanic ejecta Hazards	17090
b. Non-Thesaurus Terms	Skywaves Jindalee		

16 SUMMARY OR ABSTRACT:
(if this is security classified, the announcement of this report will be similarly classified)

During 1982 there occurred several incidents in which commercial jet aircraft suffered engine failure over Indonesia as they passed through clouds of dust injected into the stratosphere by an erupting volcano on Java. This paper presents some theoretical estimates of the detectability of such clouds using skywave radar. The results imply that detection would not be possible with the JINDALEE Stage B radar.

Security classification of this page: UNCLASSIFIED

DOCUMENT CONTROL DATA SHEET

Security classification of this page: UNCLASSIFIED

1 DOCUMENT NUMBERS	2 SECURITY CLASSIFICATION
AR Number: AR-003-732	a. Complete Document: Unclassified
Series Number: ERL-0301-TR	b. Title in Isolation: Unclassified
Other Numbers:	c. Summary in Isolation: Unclassified

3 TITLE

SKYWAVE RADAR DETECTABILITY OF VOLCANIC AEROSOLS

4 PERSONAL AUTHOR(S):

S.J. Anderson

5 DOCUMENT DATE:

August 1984

6 6.1 TOTAL NUMBER OF PAGES: 31

6.2 NUMBER OF REFERENCES: 14

7 7.1 CORPORATE AUTHOR(S):

Electronics Research Laboratory

7.2 DOCUMENT SERIES AND NUMBER

Electronics Research Laboratory 0301-TR

8 REFERENCE NUMBERS

a. Task: DEF 77/036

b. Sponsoring Agency: DEPARTMENT OF DEFENCE

9 COST CODE:

366965

10 IMPRINT (Publishing organisation)

Defence Research Centre Salisbury

11 COMPUTER PROGRAM(S) (Title(s) and language(s))

12 RELEASE LIMITATIONS (of the document):

Approved for Public Release

Security classification of this page: UNCLASSIFIED

The official documents produced by the Laboratories of the Defence Research Centre Salisbury are issued in one of five categories: Reports, Technical Reports, Technical Memoranda, Manuals and Specifications. The purpose of the latter two categories is self-evident, with the other three categories being used for the following purposes:

Reports	:	documents prepared for managerial purposes.
Technical Reports	:	records of scientific and technical work of a permanent value intended for other scientists and technologists working in the field.
Technical Memoranda	:	intended primarily for disseminating information within the DSTO. They are usually tentative in nature and reflect the personal views of the author.